



Published in final edited form as:

Circ Res. 2016 April 1; 118(7): 1091–1105. doi:10.1161/CIRCRESAHA.115.307647.

Long-Term Outcome of Administration of c-kit^{POS} Cardiac Progenitor Cells After Acute Myocardial Infarction: Transplanted Cells Do Not Become Cardiomyocytes, Structural and Functional Improvement and Proliferation of Endogenous Cells Persist for at Least One Year

Xian-Liang Tang, MD^{*}, Qianhong Li, MD, PhD^{*}, Gregg Rokosh, PhD, Santosh K. Sanganalath, MD, PhD, Ning Chen, MD, Qinghui Ou, MD, Heather Stowers, BS, Greg Hunt, BS, and Roberto Bolli, MD[✉]

Division of Cardiovascular Medicine and Institute of Molecular Cardiology, University of Louisville, Louisville, KY 40292

Abstract

RATIONALE—Cardiac progenitor cells (CPCs) improve left ventricular (LV) remodeling and function after acute or chronic myocardial infarction (MI). However, the long-term (>5 weeks) effects, potential tumorigenicity, and fate of transplanted CPCs are unknown.

OBJECTIVE—To assess the outcome of CPC therapy at 1 year.

METHODS AND RESULTS—Female rats underwent a 90-min coronary occlusion; 4 h after reperfusion, they received intracoronarily vehicle or 1 million male, syngeneic CPCs. One year later, CPC-treated rats exhibited smaller scars and more viable myocardium in the risk region, along with improved LV remodeling and regional and global LV function. No tumors were observed. Some transplanted (Y-chromosome^{POS}) CPCs (or their progeny) persisted and continued to proliferate, but they failed to acquire a mature cardiomyocyte phenotype and were too few (4–8% of nuclei) to account for the benefits of CPC therapy. Surprisingly, CPC transplantation triggered a prolonged proliferative response of endogenous cells, resulting in increased formation of endothelial cells and Y-chromosome^{NEG} CPCs for 12 months and increased formation, for at least 7 months, of small cells that expressed cardiomyocytic proteins (α -sarcomeric actin) but did not have a mature cardiomyocyte phenotype.

CONCLUSIONS—The beneficial effects of CPCs on LV remodeling and dysfunction are sustained for at least 1 year, and thus are likely to be permanent. Since transplanted CPCs do not differentiate into mature myocytes, their major mechanism of action must involve paracrine actions. These paracrine mechanisms could be very prolonged because some CPCs engraft, proliferate, and persist at 1 year. This is the first report that transplantation of any cell type in the heart induces a proliferative response that lasts at least 1 year. The results strongly support the safety and clinical utility of CPC therapy.

[✉] Address for correspondence: Roberto Bolli, M.D., Institute of Molecular Cardiology, 550 S Jackson Street, ACB Bldg, 3rd Floor, Louisville, KY 40202, Tel: (502) 852-1837, Fax: (502) 852-6474, rbolli@louisville.edu.
^{*}equal contributions as first authors

Keywords

cardiac progenitor cells; myocardial ischemia-reperfusion; cardiac repair; ventricular remodeling; myocardial regeneration

INTRODUCTION

The adult heart contains a pool of c-kit^{POS}/CD45^{NEG} cells that have been suggested to possess the properties of cardiac progenitor cells (hereafter referred to as CPCs).¹ Recent evidence indicates that the salubrious effects of transplanted (exogenous) CPCs are not mediated by differentiation into cardiac myocytes but, rather, by paracrine actions.^{2, 3} Regardless of the mechanism of action, a plethora of experimental studies from multiple laboratories has consistently shown that administration of CPCs promotes cardiac repair, attenuates left ventricular (LV) dysfunction, and improves LV remodeling in various animal models of both acute and chronic post-myocardial infarction (MI) heart failure.^{2, 4–8} In our laboratory, we have found that transplantation of CPCs exerts a panoply of salutary effects on LV structure and function in rat^{9, 10} and pig¹¹ models of chronic ischemic cardiomyopathy and in murine models of acute MI.^{12–14}

A major limitation of all of the aforementioned studies, however, is that the follow-up after cell therapy was relatively short (4–6 weeks); consequently, the long-term (>1 year) effects of CPCs on LV function and structure in experimental models of ischemic cardiomyopathy remain unknown. Similarly, the safety of CPC therapy remains uncertain because potential adverse effects, such as tumor formation, would not be expected to be evident within the 4–6 week follow-up of the studies performed to date; a longer time frame is needed to assess this possibility. For the same reason, the long-term fate of transplanted CPCs beyond the first 4–6 weeks is essentially unknown.

Another fundamental issue that remains to be clarified is the mechanism(s) that underlies the beneficial effects of CPCs.² Differentiation of transplanted CPCs into myocytes and vascular cells has been thought to play an important role¹⁵ but, as alluded to above, in our previous studies in models of ischemic cardiomyopathy we did not observe formation of adult myocytes from transplanted cells;^{9–14} however, because in all of these studies^{9, 11–14} animals were followed up for only 4–5 weeks after cell therapy, the possibility that differentiation of transplanted CPCs into mature myocytes may occur at a later time cannot be ruled out. Since we did not observe any evidence of differentiation of exogenous CPCs,^{9–14} we have proposed³ that these cells produce their salubrious effects, at least in part, by activating the pool of endogenous CPCs; however, this possibility has not been substantiated.

Thus, several fundamental issues remain to be addressed regarding CPC therapy. From a translational standpoint, before clinical implementation, it is important to assess the long-term safety of CPC therapy and establish, in a rigorous and well-controlled experimental model, whether the cardiac reparative benefits of CPC administration are transient or permanent. From a conceptual standpoint, understanding the mechanism of action of exogenous CPCs requires an effort to illuminate the long-term fate of the transplanted cells

and to establish whether or not their salubrious effects are mediated by differentiation of the transplanted cells into mature cardiac myocytes.

The present study was undertaken to elucidate these issues. Specifically, using a well-characterized rat model⁹ and a rigorous, blinded study design, we sought to determine i) whether the effects of CPCs on LV function and remodeling after MI persist for 1 year, a period that is significantly longer than the follow-up periods previously examined;^{4–14} ii) if so, whether the salutary actions of CPCs are mediated by differentiation of the cells into adult myocytes; iii) whether transplantation of exogenous CPCs elicits proliferation of endogenous CPCs and, if so, how long this response lasts; and iv) whether administration of CPCs is associated with tumor formation over a one-year follow-up. To directly compare the results of the present investigation with those of our previous studies in rats,^{9, 10} we used a similar rat model and the same dose of CPCs as in that study. To elucidate whether transplantation of CPCs promotes cell proliferation and to delineate its time-course, BrdC was administered to different subsets of animals during the 3rd, 7th, or 12th month after MI.

MATERIALS AND METHODS

All animal experiments were performed in accordance with the Guide for the Care and Use of Laboratory Animals published by the U.S. National Institutes of Health (Eighth Edition, Revised 2010) and with the guidelines of the Animal Care and Use Committee of the University of Louisville, School of Medicine (Louisville, KY, USA).

Isolation and expansion of c-kit^{POS} CPCs

c-kit^{POS} CPCs were prepared using a modification of the method described by Beltrami *et al.*¹ Briefly, adult male Fischer 344 rats (4–6 months of age) were anesthetized with sodium pentobarbital and heparinized. The heart was harvested, rinsed with ice-cold Krebs-Henseleit perfusion buffer (KH), perfused in a retrograde fashion with KH perfusion buffer at 37°C, 5 ml/min, for 6–8 min to wash out the blood, and then perfused with digestion buffer (1 mg/ml of collagenase II in KH) for 10 min. The digested heart was cut into ~1 mm³ cubes which were then triturated until cells were completely dissociated. The non-myocyte population was separated from myocytes by gravity sedimentation, counted (number of cells determined), and centrifuged at 600 g for 10 min at room temperature. The cell pellet was resuspended and the cells were seeded onto two 150 mm dishes in F12K medium with 5% FBS (HyClone), 10 ng/ml bFGF (Peprotech), and 10 ng/ml LIF (Chemicon) (RCPC medium). After six days of expansion, c-kit^{POS} cells were sorted with magnetic beads using a rabbit anti-c-kit antibody (H-300, Santa Cruz). The recovery of c-kit^{POS} CPCs was determined by flow cytometric analysis (BD LSRII, Becton–Dickinson) with an R-phycoerythrin-conjugated monoclonal anti-c-kit antibody (Pharmingen). In the sorted CPCs, expression of c-kit was repeatedly determined by flow cytometric analysis in cell passages 1 through 6. C-kit^{POS} CPCs from passages 4–6 were used in all *in vivo* studies of post-MI CPC transplantation.

Surgical preparation and experimental protocol

The protocol and dose of CPCs were similar to those used in our previous studies^{9, 10} (Fig. 1). Female Fischer 344 rats (age, 3 months; weight, 175 ± 20 g) were anesthetized with ketamine (37 mg/kg) and xylazine (5 mg/kg) and ventilated with a rodent respirator (Harvard Apparatus). Anesthesia was maintained with isoflurane inhalation and body temperature was kept at 37°C with a heating pad. After administration of antibiotics, the chest was opened and the heart exposed. All animals underwent a 90-min occlusion of the left anterior descending coronary artery followed by reperfusion, after which the chest was closed. Four hours after reperfusion, rats were reanesthetized, the chest reopened, and a thin catheter (Intracath, 22G, Becton Dickinson) was advanced into the aortic root via the left ventricular (LV) apex.¹⁶ The aorta and the pulmonary artery were occluded briefly with a snare for two 20-s intervals, 10 min apart, and vehicle or CPCs were injected into the aortic root during the occlusion.¹⁶ CPCs were suspended in sterile Plasma-Lyte A solution (1×10^6 CPCs diluted in 1 ml). All rats were euthanized 1 year later (Fig. 1). In phase A, rats were used to assess LV function and structure and for histological studies (Fig. 1A). To identify newly-formed cells, in phase B 5-bromo-2'-deoxycytidine (BrdC, MP Biomedicals, LLC), a more water-soluble precursor of 5-bromo-2'-deoxyuridine (BrdU), was infused subcutaneously with Alzet® mini-osmotic pumps (Durect Corp., CA, USA) during the 3rd, 7th, or 12th month after reperfusion (33 mg/kg/day for 1 month) (Fig. 1B).

Echocardiography

Serial echocardiographic studies were performed as described¹⁷ under light anesthesia (pentobarbital, 25 mg/kg, i.p.) 2 days before surgery and at 48 h and 3, 6, and 12 months after treatment. The anterior chest was shaved and rats were placed in the left lateral decubitus position. Body temperature was maintained between 36.9°C and 37.3°C. Echocardiographic images were obtained using an HP SONOS 7500 ultrasound system equipped with a L12-5 linear broadband and a S12 phased array transducers fitted with a 0.3 cm standoff. The heart was imaged in the parasternal short axis view at the level of the papillary muscles to obtain LV wall thickness and ejection fraction (EF), and in the parasternal long axis view to measure LV end-systolic and end-diastolic volumes (LVESV and LVEDV). All measurements were averaged in three consecutive cardiac cycles and analyzed off-line by a single blinded observer using the COMPACS image analysis software. All calculations were derived using standard formulas. LV end-systolic and end-diastolic diameters (LVESD and LVEDD) were measured from M-mode tracings obtained at the mid-papillary level and analyzed according to modified American Society for Echocardiography standards (posterior wall leading-edge to leading-edge and anterior wall trailing-edge to trailing-edge).¹⁸

Hemodynamics

Hemodynamic studies were performed at 1 year after MI, just before euthanasia.^{9, 10} Rats were anesthetized with ketamine (37 mg/kg) and xylazine (5 mg/kg), intubated, and mechanically ventilated. Anesthesia was maintained with 1% isoflurane and the core temperature kept at 37.0°C with a heating pad throughout the study. A 2F microtip pressure-volume (PV) catheter (SPR-869, Millar Instruments) was inserted into the right carotid

artery and advanced into the LV cavity. The right jugular vein was cannulated for fluid administration. After 20 min of stabilization, the PV signals were recorded continuously with an ARIA PV conductance system (Millar Instruments) coupled with a Powerlab/4SP A/D converter (AD Instruments), stored, and displayed on a personal computer. PV relations were assessed by transiently compressing the inferior vena cava with a cotton swab. Parallel conductance from surrounding structures was calculated by injecting a small bolus of 15% NaCl through the jugular vein. LV end-diastolic pressure (LVEDP), dP/dt_{max} , end-systolic elastance (Ees), and preload recruitable stroke work (PRSW) were calculated using the PVAN software program (Millar).^{9, 10}

Morphometry and histology

After the hemodynamic measurements, a polyethylene catheter filled with phosphate buffer (0.2 M, pH 7.4) and heparin (100 IU/ml) was advanced to the ascending aorta via the right carotid artery. In rapid succession, the heart was arrested in diastole by injecting 1.0 ml of a mixture of cadmium chloride (100 mM)/potassium chloride (3 M) through the aortic catheter. The heart was then excised and perfused retrogradely with phosphate buffer for ~3 min to flush out residual blood in the coronary circulation, followed by perfusion with 10% neutral buffered formalin solution for 15 min. Perfusion pressure was maintained between 60 and 80 mmHg while end-diastolic pressure was kept at 8 mmHg. After perfusion-fixation, the atria and right ventricle were dissected from the left ventricle. The LV weight was measured. The heart was cut into four transverse slices (~2-mm thick), which were processed, embedded in paraffin, sectioned at 4- μ m intervals, and stained with Masson's trichrome, picrosirius red, or antibodies against specific cell markers. Images were acquired digitally and analyzed using NIH ImageJ (1.46r). From the Masson's trichrome-stained images, morphometric parameters including risk area, scar area, and LV wall thickness in the risk were measured in each section.^{9, 10} In accordance with our previous work,⁹ the risk region was defined as the sum of the LV segment containing the infarct scar and the two border zones (defined as the regions that straddle 0.5 mm on either side of the lateral borders of the scar). To quantitate both the degree of LV dilation and the degree of infarct wall thinning, the LV expansion index was calculated.⁹ Myocardial collagen content was quantitated on the picrosirius red-stained sections by determining collagen density (as percentage of area) under polarized light.⁹

Immunohistochemistry

Immunohistochemistry was performed in formalin-fixed, paraffin-embedded, 4- μ m-thick heart sections. CPC proliferation was assessed by immunofluorescent staining of nuclei for BrdU. Myocytes were stained with α -sarcomeric actin (α -SA) antibodies and myocyte membranes were stained with FITC-conjugated wheat germ agglutinin (WGA) (Sigma) to facilitate the identification of individual myocytes for analysis of myocyte density. To determine vessel density, heart sections were stained with biotinylated Isolectin B4 (IB4) (Sigma).¹⁹ Newly-formed CPCs were evaluated by immunofluorescent staining of cell membranes for c-kit and CD45 (Santa Cruz) and staining of nuclei for BrdU on the same heart sections.⁹

Fluorescent *in situ* hybridization (FISH) analysis

To check the fate of the transplanted male CPCs, single-labeled Y chromosome was detected by fluorescence *in situ* hybridization (FISH) according to the modified manufacturer's protocol (ID Labs, London, ON).^{20, 21} Serial tissue sections from paraffin-embedded heart blocks were cut to 4- μ m thickness. Heart tissue sections on coated slides were deparaffinized in xylene and rehydrated gradually, followed by an antigen retrieval procedure. After treatment with pepsin and air-drying, a denatured rat Y chromosome probe was added to each section and covered by coverslip. After overnight hybridization at RT°C, the coverslip was removed and serial washings were performed. Male and female rat heart tissue sections were used as positive and negative controls, respectively, in the FISH staining procedure. The fate of transplanted CPCs in the heart was assessed by double staining with a green fluorochrome-labeled Y-chromosome probe and a specific monoclonal antibody against the cardiac-specific marker α -sarcomeric actin (Sigma). Nuclei were counterstained with DAPI. To minimize auto fluorescence, slides were incubated with 0.1% Sudan Black B (Sigma), rinsed in PBS, and then mounted with ProLong Gold antifade reagent (Invitrogen).¹³ Immunohistochemical signals were imaged by confocal microscopy and quantitatively analyzed by Image J (1.46, NIH). In each heart, Y-chromosome^{POS} nuclei, Y-chromosome^{POS} nuclei/ α -sarcomeric actin^{POS} cells, and total nuclei were counted in 25 confocal images (6 from the scar region, 14 from two border zones, and 5 from the noninfarcted region), and the results were corrected for the Y-chromosome density detected in normal male myocardium. For Y-chromosome^{POS} nuclear analysis, an average of 1,235 nuclei was counted in a 0.352 mm² area per rat heart and the results were normalized to male heart Y-chromosome density.

Statistical analysis

All data are expressed as means \pm SEM. Intragroup and intergroup comparisons of the echocardiographic and BrdU data were performed using a two-way ANOVA with repeated measures followed by the Student's *t*-test with Bonferroni correction. Intergroup comparisons of morphometric, histologic, immunohistochemical, and hemodynamic data were performed by one-way ANOVA followed by the Student's *t*-test with the Bonferroni correction. All analyses were conducted with SigmaStat 3.5. Values of $P < 0.05$ were considered significant.

RESULTS

Characterization of rat c-kit^{POS} CPCs

C-kit^{POS} CPCs to be used for transplantation were isolated by magnetic activated cell sorting (MACS) from a non-myocyte cell population obtained from syngeneic rat hearts. The recovery of c-kit^{POS} cells ranged from 0.2 - 3.0% of the total cell population, averaging $0.71 \pm 0.17\%$ (n=18). After expansion and sorting, c-kit^{POS} CPCs accounted for ~80% of cells (Fig. 2A and B) and the percentage of c-kit^{POS} cells remained stable through four passages in culture (Fig. 2C).

Exclusions

A total of 142 rats were enrolled in this study. Four normal (noninfarcted) rats were used as a reference for comparison; these animals did not undergo MI, received BrdC infusion for 1 month, and had age equivalent to the 12th month subgroups in the cohorts subjected to MI (Fig. 1).

The remaining 138 rats were subjected to MI and studied in two consecutive phases (A and B [Fig. 1]). In Phase A, 90 rats (40 in the vehicle-treated and 50 in the CPC-treated group) were used to assess the long-term effects of CPCs, both with respect to LV function and structure and with respect to tumor formation (Fig. 1). Of these 90 rats, 22 (10 in the vehicle group and 12 in the CPC-treated group) died at various times during the 1 year follow-up, while 68 (30 in the vehicle-treated and 38 in the CPC-treated group) survived till the end of the 1-year follow-up. The 1-year survival rate was similar between the two groups (Supplementary Fig. 1). Postmortem examination of the 50 CPC-treated rats (12 of which died during follow-up while 38 survived till the end of the 1-year follow-up) did not yield any evidence of tumor formation. Among the 68 rats that survived for 1 year, a subset of 26 (12 in the vehicle-treated and 14 in the CPC-treated group) were used for serial echocardiographic analyses and for pathological/histological studies.

In Phase B, 48 rats (24 in the vehicle-treated and 24 in the CPC-treated group) were used for studies of BrdU incorporation (Fig. 1). Twelve rats died during the period of BrdC infusion (six in the vehicle-treated and six in the CPC-treated group); therefore, six rats completed the protocol in each of the three subgroups (BrdC infusion during the 3rd, 7th, and 12th month after MI) in both the control and treated groups.

Body weight, LV size, and gross pathology

Although body weight was similar between the two groups at baseline, the gain in body weight was significantly greater in the CPC group at 3, 6, and 12 months after MI (Table 1). Postmortem measurements of LV size showed that the length and weight of the left ventricle were significantly increased in both groups compared with normal controls of similar age (Table 1); however, LV length and weight were significantly less in the CPC-treated vs. the vehicle-treated group, concomitant with a reduced LV/body weight ratio, indicating less LV hypertrophy (Table 1). Gross pathologic examination did not reveal any tumors.

Morphometric analysis

Despite similar risk regions ($35.7 \pm 1.8\%$ of LV weight in the vehicle-treated group vs. $35.3 \pm 2.6\%$ in the CPC-treated group) (Table 2 and Fig. 3B), in CPC-treated rats scar size was reduced ($11.6 \pm 1.2\%$ of LV weight vs. $16.6 \pm 1.1\%$ in the vehicle group, $P < 0.01$) (Figs. 3A and B) while the amount of viable tissue within the risk region was increased ($65.8 \pm 3.0\%$ of risk region weight vs. $53.6 \pm 2.4\%$ in the vehicle group, $P < 0.01$) (Table 2 and Figs. 3A and B), suggesting that the infusion of CPCs resulted in formation of new myocardium in the infarcted region. The total amount of viable tissue in the left ventricle, expressed in absolute units, was similar in CPC- and vehicle-treated hearts (914.3 ± 29.8 and 995.8 ± 30.3 mg, respectively); however, since total LV weight tended to be higher in vehicle-treated hearts, the percentage of LV weight that was accounted for by viable tissue

was slightly, but significantly, greater in CPC-treated hearts ($88.4 \pm 1.2\%$ vs. $83.4 \pm 1.1\%$ in the vehicle group, $P < 0.01$) (Table 2 and Fig. 3B). In addition, CPC-treated rats exhibited an increase in the thickness of the infarcted LV wall and a decrease in the LV expansion index ($P < 0.05$ for both) (Figs. 3A and B).

Because myocardial fibrosis plays a key role in the pathology of LV remodeling after MI,^{22, 23} we examined whether CPCs attenuated myocardial collagen deposition. Collagen content in the risk region was significantly less in CPC-treated rats compared with vehicle-treated rats ($P < 0.05$), although there was no significant difference between the two groups in the posterior wall (noninfarcted region) (Supplementary Fig. 2). This reduced collagen deposition in the myocardium may have contributed, at least in part, to the functional benefits of CPC therapy.

Myocyte and vessel density

Myocyte density and myocyte nuclear density were assessed by staining myocytes with α -SA antibodies and myocyte membranes with FITC-conjugated WGA to facilitate counting individual myocytes (Supplementary Fig. 4). Of these two parameters, myocyte density may be a more reliable indicator of the number of myocytes per area unit because it is independent of the number of nuclei per cell. We deliberately excluded from the counts small cells that lacked the morphology of mature cardiomyocytes. In the risk region, both myocyte density and myocyte nuclear density were significantly higher in CPC-treated rats compared with vehicle-treated rats. Similar trends were observed in the noninfarcted region, but the differences were not statistically significant (Supplementary Fig. 4). Although other explanations are possible, increased myocyte density in CPC-treated hearts is consistent with formation of new myocytes.

Vascular density was assessed by staining tissue with FITC-conjugated isolectin B4 in rats that received BrdU infusion during the 12th month after MI (Supplementary Fig. 3). Presumably as a result of scarring, vascular density was significantly less in the risk region than in the noninfarcted region of both vehicle- and CPC-treated hearts (Supplementary Fig. 3C). In the noninfarcted region, vascular density tended to be greater in CPC-treated than in vehicle-treated rats, but the difference was not statistically significant (Supplementary Fig. 3C). In the risk region, total vascular density was similar; however, further analysis revealed that the density of BrdU^{POS} vessels and BrdU^{POS} endothelial cells was significantly higher in CPC-treated rats than in vehicle-treated rats (Supplementary Figs. 3D–F). No such differences were observed in the noninfarcted region. These data suggest that treatment with CPCs increased the turnover of endothelial cells in the risk region.

Interestingly, the distribution of vessel diameter was significantly different between the vehicle-treated and the CPC-treated groups: the former exhibited a greater number of vessels between 10–50 micrometer in diameter, both in the risk region and in the noninfarcted region (Supplementary Figs. 3G–K).

Echocardiographic and hemodynamic analysis

The echocardiographic data are summarized in Figs. 4A and B. At 48 h after MI, all parameters of LV function and dimensions, measured by echocardiography, were similar in the control and treated groups (Fig. 4B), indicating that the extent of injury was comparable.

As expected, vehicle-treated rats exhibited a progressive increase in LV end-systolic and end-diastolic volumes (Fig. 4B), indicative of post-MI LV remodeling. Remarkably, both of these changes were essentially abrogated in CPC-treated rats, in which LV end-systolic and end-diastolic volumes did not increase appreciably from 48 h to 12 months post-MI; as a result, LV volumes were significantly less in treated than controls rats at 3, 6, and 12 months post-MI. At 12 months, both groups exhibited greater end-systolic and end-diastolic volumes than normal (noninfarcted), age-matched rats, but the increase was less in CPC-treated rats (Fig. 4B). In the CPC-treated group, the thickness of the infarcted (anterior) LV wall in diastole increased following administration of CPCs, so that at 3, 6, and 12 months after MI it was significantly greater than in vehicle-treated rats, although at 12 months it was still less than in normal (non-infarcted) rats. End-diastolic thickness of the posterior (noninfarcted) wall did not differ between the two groups.

At 48 h after MI, the degree of regional and global LV systolic dysfunction, assessed by systolic thickening fraction, fractional shortening, and LVEF, was similar in the two groups (Fig. 4B), indicating that the extent of injury sustained during coronary occlusion/reperfusion was comparable. In control rats, these parameters of regional and global LV systolic function exhibited a progressive deterioration throughout the 12-month follow-up, consistent with the development of post-MI cardiomyopathy (Fig. 4B). In rats treated with CPCs, however, the deterioration in both regional and global LV function was attenuated (Fig. 4B). For example, thickening fraction in the anterior (infarcted) LV wall was significantly ($P<0.05$) greater in treated than vehicle-treated rats at 6 months ($78.6 \pm 3.0\%$ vs. $66.7 \pm 4.0\%$, respectively, $P<0.05$) and 12 months of follow-up ($71.1 \pm 3.3\%$ vs. $57.6 \pm 3.7\%$, $P<0.05$) (Fig. 4B). The preservation of thickening fraction in the anterior LV wall of CPC-treated rats was such that at 12 months this parameter did not differ significantly from normal (noninfarcted) age-matched rats (Fig. 4B). Similarly, LVEF was significantly greater in treated than control rats at 3 months ($76.0 \pm 1.5\%$ vs. $66.0 \pm 2.9\%$, respectively, $P<0.01$), 6 months ($73.2 \pm 2.6\%$ vs. $62.2 \pm 2.5\%$, $P<0.01$), and 12 months of follow-up ($70.8 \pm 2.2\%$ vs. $62.9 \pm 2.8\%$, $P<0.01$). Taken together, the echocardiographic data indicate that treatment with CPCs markedly attenuated LV dilation and regional and global dysfunction throughout the duration of the study.

Consistent with the echocardiographic data, hemodynamic studies (performed before euthanasia using a Millar conductance catheter) demonstrated that LV function was significantly improved by the administration of CPCs (Fig. 4C). At 12 months after MI, compared with control rats, CPC-treated rats exhibited a significant decrease in LV end-diastolic pressure and a significant increase in both load-dependent parameters of LV performance, such as LVEF and maximal and minimal LV dP/dt, and load-independent parameters, such as increased preload recruitable stroke work and end-systolic elastance (Fig. 4C).

Analysis of BrdU positivity

To delineate the proliferative response of the heart to MI and CPC transplantation, in Phase B we infused BrdC for 30 days during the 3rd, 7th, and 12th month post-MI. In the risk region, at all three time periods examined (3rd, 7th, and 12th month), the total number of BrdU^{POS} cells was markedly increased compared with the posterior wall (noninfarcted region) in the same hearts and compared with normal (noninfarcted), age-matched rats that received BrdC at an age equivalent to the 12th month after MI in the infarcted rats (Figs. 5A and B), indicating that MI promotes sustained cell proliferation in the infarcted region that lasts at least 12 months. The total number of BrdU^{POS} cells was highest in the third month post-MI and then declined progressively, but even in the 12th month, it was still much higher (almost 10-fold) than in normal (noninfarcted) rats (Fig. 5B). In the posterior wall (noninfarcted region), the proliferative response was less pronounced and more short-lived, both in CPC-treated and control rats: in both groups, the total number of BrdU^{POS} cells was higher than in the normal (noninfarcted) rats during the 3rd month post-MI but not during the 7th or 12th month (Fig. 5B), indicating that the cellular proliferation induced by MI in noninfarcted LV regions subsided between 3 and 7 months. There was no significant difference in the total number of BrdU^{POS} cells between the control and CPC-treated groups at any time point, either in the risk region or in the noninfarcted region (Fig. 5B). Thus, total cellular proliferation was not affected by CPC administration.

Co-staining of tissue with BrdU and α -SA antibodies revealed that, compared with normal (noninfarcted) rats, the number of double positive (BrdU^{POS}/ α -SA^{POS}) cells was significantly increased in the risk region in the 3rd, 7th, and 12th month and in the noninfarcted region in the 3rd and 7th month post-MI, suggesting increased formation of new cells that expressed cardiomyocytic proteins (Fig. 5C). This increase occurred in both CPC-treated and vehicle-treated (control) rats (Fig. 5C). However, in contrast to the total number of BrdU^{POS} cells, there were significant differences between the two groups: Compared with vehicle-treated rats, CPC-treated rats exhibited a greater number of double positive (BrdU^{POS}/ α -SA^{POS}) cells in the risk region in the 3rd month (+105%, $P<0.05$) and 7th month (+122%, $P<0.05$) and in the noninfarcted region in the 3rd month (+66%, $P<0.05$) (Fig. 5C). These data suggest that transplantation of CPCs promotes formation of new cells expressing cardiomyocyte markers for at least 7 months in the risk region and for at least 3 months in the noninfarcted region. It is important to point out, however, that even at 1 year the double positive (BrdU^{POS}/ α -SA^{POS}) cells did not exhibit the phenotype of mature cardiomyocytes: they were small and lacked organized sarcomeric structure (Fig. 5A). In fact, very few, in any, BrdU^{POS} mature cardiomyocytes were observed at any time point (3rd, 7th, and 12th month) in either treatment group. Therefore, the double positive (BrdU^{POS}/ α -SA^{POS}) cells cannot be considered cycling myocytes or myocyte precursors.

Analysis of Y-chromosome^{POS} cells

To assess the fate of transplanted male CPCs, the number of Y-chromosome^{POS} cells was measured by FISH at 1 year after transplantation. The advantage of using the Y-chromosome to track transplanted cells in long-term studies is that, unlike EGFP or beta-galactosidase, its presence is not affected by changes in gene expression.^{24–26} Y-chromosome^{POS} cells were still detectable at 1 year after transplantation: they were more abundant in the risk region

($7.7 \pm 1.2\%$ of total nuclei) than in the noninfarcted region ($3.8 \pm 0.9\%$) (Figs. 6A–E and G). Similarly, double positive (Y-chromosome^{POS}/α-SA^{POS}) cells were found predominantly in the risk region ($4.8 \pm 0.9\%$ of the nuclei vs. $0.5 \pm 0.2\%$ in the noninfarcted region) (Fig. 6A–E and H). The ratio of Y-chromosome^{POS}/α-SA^{POS} cells to total Y-chromosome^{POS} cells in the risk region was $62.2 \pm 2.1\%$ (Fig. 6I), suggesting that most surviving CPCs (or their progeny) expressed cardiomyocytic proteins. However, in absolute terms, the number of double positive (Y-chromosome^{POS}/α-SA^{POS}) cells was low, as indicated above ($4.8 \pm 0.9\%$ of nuclei in the risk region and $0.5 \pm 0.2\%$ in the noninfarcted region) (Fig. 6H). Furthermore, these cells did not resemble mature myocytes: most were mononucleated and small, without a sarcomeric structure, resembling late fetal/neonatal cells; mature, large Y-chromosome^{POS} myocytes were found only rarely in the risk region (white arrows in Figs. 6B and 6D). In summary, these data indicate that some transplanted CPCs (or their progeny) persisted at 1 year after intracoronary delivery. In the risk region, most of these cells expressed cardiac proteins (α-SA) but, even after 1 year, failed to acquire a mature myocyte phenotype; furthermore, their number ($<5\%$ of nuclei) was not sufficient to account for the functional improvement observed.

Analysis of newly-formed CPCs

The failure of transplanted CPCs to differentiate into mature myocytes implies that these cells improved LV function via paracrine mechanisms. One such potential mechanism is activation of endogenous CPCs. To test this hypothesis, we measured the number of c-kit^{POS} cells at 1 year after transplantation, separating those of hematopoietic origin (which are c-kit^{POS}/CD45^{POS}) from CPCs (which are c-kit^{POS}/CD45^{NEG}) (Figs. 7A–G and Supplementary Fig. 6). The total number of c-kit^{POS} cells in both the risk and noninfarcted regions was similar in CPC-treated and control rats (Fig. 7H). When the number of CPCs (c-kit^{POS}/CD45^{NEG} cells) was expressed as a percent of total c-kit^{POS} cells, it was significantly higher in CPC-treated animals ($47.6 \pm 7.0\%$ of total c-kit^{POS} cells vs. $27.9 \pm 4.1\%$ in the risk region, $P < 0.05$; $61.9 \pm 14.0\%$ vs. $38.7 \pm 14.6\%$ in the noninfarcted region, Fig. 7I). However, when the number of CPCs (c-kit^{POS}/CD45^{NEG} cells) was calculated as a percent of total nuclei, it did not differ significantly in the two groups, although it was higher in CPC-treated animals (Fig. 7J). Thus, calculation of static CPC numbers did not reveal a significant effect of CPC transplantation on the abundance of CPCs in the myocardium 1 year later.

Analysis of CPC turnover, however, yielded different results. The total number of new c-kit^{POS} cells (c-kit^{POS}/BrdU^{POS} cells) formed during the 12th month after MI, expressed as a percent of total nuclei, was similar in the two groups (Fig. 7K). However, the number of new CPCs formed during the 12th month after MI (c-kit^{POS}/CD45^{NEG}/BrdU^{POS} cells), expressed as a percent of total nuclei, was higher in CPC-treated than in control rats ($3.9 \pm 0.6\%$ vs. $1.1 \pm 0.3\%$ in the risk region, $P < 0.01$; $3.5 \pm 0.8\%$ vs. $1.6 \pm 0.9\%$ in the noninfarcted region, $P = 0.132$) (Fig. 7L). In addition, in CPC-treated rats, the new CPCs (c-kit^{POS}/CD45^{NEG}/BrdU^{POS} cells) constituted a greater percentage of total CPCs (c-kit^{POS}/CD45^{NEG} cells) than in control rats: $47.4 \pm 4.8\%$ vs. $21.9 \pm 5.2\%$ in the risk region, $P < 0.01$; $54.8 \pm 7.8\%$ vs. $36.4 \pm 16.0\%$ in the noninfarcted region) (Fig. 7M). Taken together, these data indicate that, at 1 year after CPC administration, the formation of new CPCs was increased in CPC-treated hearts compared with vehicle-treated hearts, particularly in the risk region.

Next, we sought to determine whether the newly-formed CPCs derived from exogenous (Y-chromosome^{POS}) or endogenous (Y-chromosome^{NEG}) cells. To this end, we examined the presence of Y-chromosome in c-kit^{POS}/BrdU^{POS} cells (Fig. 8A and Supplementary Fig. 7A–C). We found that proliferation of Y-chromosome^{POS} cells was still robust at 12 months after transplantation, since newly-formed Y-chromosome^{POS} cells (Y-chromosome^{POS}/BrdU^{POS} cells) constituted $29.0 \pm 3.2\%$ and $19.2 \pm 6.5\%$ of total Y-chromosome^{POS} nuclei in the risk and noninfarcted region, respectively (Fig. 8B). The number of newly-formed Y-chromosome^{POS} cells was significantly higher in the risk region than in the noninfarcted region ($2.5 \pm 0.3\%$ of total nuclei vs. $1.2 \pm 0.4\%$, respectively) (Fig. 8F).

With regard to c-kit expression, at 1 year after transplantation, only a small fraction of Y-chromosome^{POS} cells were c-kit^{POS} ($14.0 \pm 2.5\%$ in the risk region and $6.7 \pm 3.7\%$ in the noninfarcted region) (Fig. 8D), indicating that most transplanted cells and their progeny had lost c-kit positivity, presumably as a result of differentiation into more mature phenotypes. Importantly, Y-chromosome^{POS}/c-kit^{POS} cells constituted only $1.0 \pm 0.2\%$ of total nuclei in the risk region and $0.5 \pm 0.3\%$ in the noninfarcted region (Fig. 8E); these percentages were much lower than the percentages of CPCs (c-kit^{POS}/CD45^{NEG} cells) ($6.6 \pm 1.0\%$ and $5.3 \pm 1.4\%$ of total nuclei in the risk and noninfarcted regions, respectively, Fig. 7J). Similarly, the number of new Y-chromosome^{POS}/c-kit^{POS} cells formed during the 12th month after MI (Y-chromosome^{POS}/c-kit^{POS}/BrdU^{POS} cells) was much lower than the number of new CPCs (c-kit^{POS}/CD45^{NEG}/BrdU^{POS} cells) formed during the 12th month after MI in the risk region ($0.9 \pm 0.2\%$ of total nuclei [Fig. 8C] vs. $3.9 \pm 0.6\%$ of total nuclei, Fig. 7L) as well as in the noninfarcted region ($0.5 \pm 0.3\%$ of total nuclei [Fig. 8C] vs. $3.5 \pm 0.8\%$ of total nuclei [Fig. 7L]). Thus, even if all of the Y-chromosome^{POS}/c-kit^{POS} cells were CPCs (which is unlikely), they would be a small fraction (~20% or less) of both total CPCs and newly-formed CPCs, implying that neither the majority of CPCs nor the majority of newly-formed CPCs was derived from the transplanted (Y-chromosome^{POS}) cells. These data indicate that the increased proliferation of CPCs observed 1 year after CPC transplantation cannot be accounted for by proliferation of transplanted CPCs, and therefore must involve primarily endogenous cells.

DISCUSSION

Although the ability of CPCs to alleviate LV dysfunction and remodeling has been demonstrated by several laboratories,^{2, 4–8, 10} no previous study has examined the long-term outcome of CPC therapy - an issue that is obviously fundamental from a translational standpoint. Thus, at the preclinical level, the duration of the salubrious effects of CPC therapy and its potential tumorigenic effects remain unknown. Furthermore, no information is available regarding the long-term fate of transplanted CPCs, which hinders elucidation of their mechanism(s) of action.

The present study is unique because of its long (1 year) follow-up after CPC administration. Our results provide several new findings that are important from both a conceptual and a therapeutic standpoint: i) the beneficial effects of CPCs on regional and global LV function after acute MI are sustained for at least 1 year, and thus, are likely to be permanent; ii) CPC therapy also affords a sustained (1 year) improvement in LV remodeling, as evidenced by a

reduction in LV dilatation, LV hypertrophy, myocardial fibrosis in the risk region, and LV expansion index; iii) transplantation of CPCs is not associated with any evidence of tumor formation over the ensuing 12 months; iv) at 12 months after CPC administration, the risk region exhibits an increase in viable myocardium and myocyte density, both of which suggest (but do not prove) myocyte regeneration; v) some transplanted CPCs (or their progeny) engraft and persist at 1 year after transplantation, but they fail to acquire a mature cardiomyocyte phenotype and their number (4–8% of nuclei) is insufficient to account for the functional and structural benefits of CPC therapy, implying that the major mode of action of CPCs is via paracrine actions; vi) transplantation of exogenous CPCs triggers a robust and surprisingly sustained proliferative response of endogenous cells that is still present 12 months later; vii) a major component of this proliferative response is the formation of new cells that express cardiomyocytic proteins (α -SA) but do not have a mature cardiomyocyte phenotype; viii) an additional component is the increased formation of new vessels in the risk region which, however, is not associated with increased vascular density; ix) the CPC-induced proliferative response includes also increased formation of new CPCs, which is still evident at 12 months after CPC administration; and x) although the transplanted (Y-chromosome^{POS}) cells continue to proliferate briskly at 12 months, the increased formation of new CPCs observed at this time cannot be accounted for by proliferation of exogenous (Y-chromosome^{POS}) CPCs, and thus must result from activation of endogenous (Y-chromosome^{NEG}) cells. Taken together, these results offer new important insights into the long-term effects and mechanism of action of CPC therapy, and have important implications for therapeutic translation.

Every effort was made to ensure that the conclusions of this study were supported by robust data. Sample sizes were relatively large. LV function was carefully addressed with two independent techniques. The results were analyzed by investigators that were blind to treatment. Furthermore, LV function was assessed using multiple parameters, including measures of regional and global function and load-dependent and independent indices. An exhaustive immunohistological analysis was performed to quantify the frequency of selected antigens. In each heart, an average of 1,702 nuclei was counted and twenty-five confocal microscopic fields were examined for measurements of BrdU, WGA, IB4, α -SA, c-kit, CD45, and Y-chromosome positivity.

An important goal of this study was to evaluate, in a careful and systematic manner, the possible tumorigenic actions of exogenous CPCs. To accomplish this goal, we studied 50 rats that received CPCs and were followed for 1 year. At postmortem examination, we found no evidence of tumor formation in any of these animals, or in any of the other animals used for the functional and structural analyses, indicating that transplantation of CPCs, at least when done within the first five passages (as in this study), is not tumorigenic.

One of the most striking results of this investigation is the magnitude of the salubrious effects produced by a single administration of CPCs. There was a significant improvement in global LV systolic function, as documented by two independent methods (echocardiographic and hemodynamic studies) and by a multitude of parameters, both load-dependent and load-independent (Fig. 4). Regional function in the infarcted region was also ameliorated (Fig. 4B), presumably as a result of the greater proportion of viable tissue in this region and the

increased wall thickness (Fig. 3). Another important benefit of CPC therapy was the reduction in LV hypertrophy (Table 1), which probably resulted from the functional improvement effected by CPCs. The reduction in collagen content observed in the risk region (Supplementary Fig. 2) may be the consequence of both increased myocyte regeneration (as suggested by the increased amount of viable tissue in the risk region [Figs. 3A and B]) and favorable effects of CPCs on the extracellular matrix. A decrease in collagen is not only a marker of reduced cardiac injury but also a potential mechanism for improved cardiac performance.

Perhaps the most important question regarding the benefits imparted by CPCs pertains to their mechanism of action.² Previous studies from our lab have shown that when CPCs were transplanted into injured hearts, they gave rise to cells that expressed myocyte-specific proteins (such as α -SA) but were small and did not resemble adult myocytes.^{2, 3, 9–11, 13} Furthermore, the number of cells derived from exogenous CPCs was insufficient to explain the improvement in cardiac function;^{2, 3, 9–11, 13} for example, <3% of transplanted CPCs could be found in the mouse heart at 35 days after adoptive transfer (a time when cardiac performance was enhanced)^{12, 27} and intracoronary infusion of CPCs promoted myocardial repair in rat and porcine models of chronic ischemic cardiomyopathy despite the persistence of a very low number of transplanted cells.^{9–11} In other studies, however, particularly in models of acute MI, the magnitude of CPC differentiation into adult myocytes has been reported to be substantial.^{1, 4, 28} As a consequence of these discrepant results, two different schools of thought have emerged: one that asserts that the beneficial effects of CPCs are underlain by the differentiation of transplanted cells into new vascular cells and mature myocytes,^{29, 30} and another that asserts that transplanted CPCs produce their salubrious effects via paracrine mechanisms because they do not differentiate into adult myocytes and most of them disappear shortly after adoptive transfer.^{2, 3}

The present study provides important new information that sheds light on this issue. In Phase A we found that, after administration of Y-chromosome^{POS} CPCs, robust structural and functional benefits persisted for one year despite the fact that only $7.7 \pm 1.2\%$ of nuclei were Y-chromosome^{POS} in the risk region and $3.8 \pm 1.0\%$ in the noninfarcted region at 1 year (Fig. 6G). The number of Y-chromosome^{POS} cells expressing cardiac proteins (α -SA^{POS} cells) was even lower (Fig. 6I). Furthermore, Y-chromosome^{POS} cells with a morphology resembling adult myocytes were rarely observed, if ever (Fig. 6A–D). These findings demonstrate that, with possible rare exceptions, exogenous CPCs do not differentiate into mature myocytes, even at 1 year after transplantation. Consequently, the remarkable improvement in LV function and remodeling observed at 1 year (Figs. 3 and 4) cannot be accounted for by differentiation of exogenous CPCs into new functional myocytes; the major mechanism of action must involve paracrine mechanisms on the host cells.

Nevertheless, the finding of persistent Y-chromosome^{POS} cells is noteworthy. Contrary to previous proposals,^{31, 32} our data show that transplanted CPCs (or their progeny) are not completely cleared from the heart, even after 1 year (Figs. 6 and 8), and continue to proliferate robustly at this time (Fig. 8B). This rather surprising observation raises the intriguing possibility that the paracrine actions of transplanted cells may be sustained for very prolonged periods of time after a single administration. The nature and function of

engrafted Y-chromosome^{POS} cells are unclear. At 1 year, most of these cells (>85%) have lost c-kit expression (Fig. 8D); 62.2±2.1% express cardiac proteins (α-SA) in the risk region and 14.0±6.4% in the noninfarcted region (Fig. 6I), although they fail to acquire a mature myocyte phenotype (Fig. 6A–D). Further studies will be necessary to determine whether the engraftment of Y-chromosome^{POS} cells is an epiphenomenon or is necessary for the LV functional improvement to occur.

It is unlikely that the Y-chromosome^{POS} cells were the result of fusion of transplanted CPCs with endogenous cells, such as myocytes, because fusion would be expected to produce binucleated cells of size comparable to the original cells and fusion events are rare (<1:10⁴–10⁵ cells^{33, 34}); in contrast, the Y-chromosome^{POS} cells we observed were very small, mononucleated, and relatively frequent (Fig. 6A–D). Fusion has never been reported for CPCs. Engulfment of transplanted CPCs by macrophages is also unlikely because the Y-chromosome of engulfed cells would not be localized to the nucleus and, in any case, would disappear as a result of DNA degradation, particularly after 1 year.

One potential paracrine action of transplanted CPCs would be activation of endogenous cells. To determine whether infusion of exogenous CPCs elicits proliferation of endogenous cells and, if so, what the time-course is, in Phase B of the study we administered BrdC for one month during the 3rd, 7th, or 12th month after MI. These experiments led to the remarkable finding that, in CPC-treated rats, a single infusion of cells resulted in a prolonged proliferative response within the host myocardium, which persisted for at least 12 months in the risk region and 3 months in the noninfarcted region and was manifested in the formation of new cells that expressed cardiac-specific proteins, such as α-SA (BrdU^{POS}/α-SA^{POS} cells) (Fig. 5). The nature of these cells remains unclear; although the expression of α-SA would suggest differentiation toward a cardiomyocytic lineage, the cells were small and did not acquire the phenotype of mature myocytes, even after 12 months (Fig. 5). Indeed, although we examined all three subgroups of rats that received BrdC (infusion of BrdC in the 3rd, 7th, and 12 month after MI), we observed few, if any, BrdU^{POS} mature myocytes in any of these subgroups. Therefore, the double positive (BrdU^{POS}/α-SA^{POS}) cells that we found (Fig. 5) cannot be regarded as cycling myocytes or myocyte precursors. Further studies will be necessary to ascertain their nature. As was the case for the rest of the proliferative response, the CPC-induced proliferation of BrdU^{POS}/α-SA^{POS} cells involved both the infarcted and the noninfarcted regions but was more robust in the former (Fig. 5). The CPC-induced proliferation also resulted in increased formation of endothelial cells in the risk region; vessel density was not augmented, however, suggesting increased turnover of endothelial cells (Supplementary Fig. 3F).

Having observed that infusion of exogenous CPCs induced a surprisingly prolonged proliferative response of small α-SA^{POS} cells and endothelial cells, we investigated whether this phenomenon was associated with activation and proliferation of CPCs (c-kit^{POS}/CD45^{NEG} cells). We found that, at 1 year after transplantation, the total number of CPCs was not significantly different in vehicle- and CPC-treated rats (Fig. 7H). However, the turnover of CPCs was significantly increased in CPC-treated rats, because the frequency of c-kit^{POS}/CD45^{NEG} cells that were BrdU^{POS} (i.e., formed during the 12th month after MI) was greater than in control rats, both when they were expressed as a percentage of total

nuclei (Fig. 7L) and of total CPCs (Fig. 7M). Previous studies have suggested that exosomes produced by various stem/progenitor cells activate endogenous CPCs.³⁵ The fact that CPCs proliferated at a higher rate, yet the total number of these cells did not increase, suggests a shortened cell life span, possibly due to increased differentiation and/or increased cell death.

What is the source of this proliferation? We were able to demonstrate that the vast majority of the proliferating (newly formed during the 12th month after MI) CPCs were endogenous because Y-chromosome^{POS} /c-kit^{POS} cells (Fig. 8E) were <20% of the CPCs (Fig. 7J), and newly-formed Y-chromosome^{POS}/c-kit^{POS} cells (Y-chromosome^{POS}/c-kit^{POS}/BrdU^{POS} cells) (Fig. 8C) were <25% of total newly-formed CPCs (c-kit^{POS}/CD45^{NEG}/BrdU^{POS} cells) (Fig. 7L). Even if one assumes that all Y-chromosome^{POS} /c-kit^{POS} cells were CPCs (which is not plausible), the majority (<75%) of the CPCs and newly-formed CPC at 12 months were not Y-chromosome^{POS}.

Beside the striking proliferative response, we found circumstantial evidence that CPC administration promoted myocyte regeneration in the risk region. Specifically, this region contained a greater percentage of viable tissue in CPC-treated vs. vehicle-treated rats (65.8 % vs. 53.6 %, respectively [Fig. 3]) and was more densely populated with mature myocytes, as evidenced by an increase in myocyte density (Supplementary Fig. 4) – two observations that would be consistent with regeneration of myocytes, although other explanations are also possible. If new mature myocytes were formed, their origin is unclear. Given that transplanted CPCs failed to acquire a mature cardiomyocyte phenotype, any new myocytes must be derived from endogenous cells, e.g., from differentiation of endogenous CPCs or other precursor cells. If such differentiation took place, it must have occurred in the absence of steady proliferation of precursor cells because, as mentioned above, we found almost no BrdU^{POS} mature myocytes irrespective of when BrdC was administered (3rd, 7th, or 12th months after CPC therapy), indicating that the endogenous cells that gave rise to mature myocytes (myocyte precursors) did not proliferate during those three months. It is possible, however, that the myocyte precursors may have proliferated in other months, when BrdC was not infused.

In conclusion, this is the first long-term study of CPCs. Our results demonstrate that the salutary effects of these cells on LV function and remodeling after MI persist for at least 1 year and, therefore, are likely to be permanent. This sustained improvement is not associated with tumor formation. The beneficial effects of CPCs cannot be explained by differentiation of transplanted cell into cardiac myocytes and, therefore, must reflect paracrine actions. Our finding that some transplanted cells are still present, and continue to proliferate, at 1 year (constituting 4–8% of the nuclei) raises the possibility that their paracrine actions may be much longer-lasting than previously thought. Surprisingly, we found that a single administration of CPCs causes a robust and sustained proliferative response leading to formation of endothelial cells and small cells that express cardiac proteins (α -SA). The exact nature of these latter cells is unclear, but they do not resemble adult cardiomyocytes, even at 12 months after CPC transplantation, and thus cannot be considered cycling myocytes or myocyte precursors. The formation of small α -SA^{POS} cells is associated with increased proliferation of endogenous CPCs that is still demonstrable 12 months after CPC infusion. To our knowledge, this is the first evidence that transplantation of cells (of any type) in the

heart induces a sustained proliferative response that lasts at least 12 months. While the mechanism for this phenomenon remains to be elucidated, its occurrence offers a plausible explanation for the seemingly paradoxical observation that the salutary effects of cell therapy persist even after the transplanted cells have disappeared. The data are consistent with a paradigm in which exogenous CPCs activate endogenous CPCs and other cells (e.g., endothelial cells and small cells expressing cardiac proteins), which proliferate and promote cardiac repair. Further research is warranted to elucidate the mechanism(s) whereby injection of CPCs triggers such a strikingly long-lasting proliferative response and the significance thereof. Meanwhile, the long-term safety and efficacy of CPCs observed in this study provide a strong rationale for clinical translation.

Supplementary Material

Refer to Web version on PubMed Central for supplementary material.

Acknowledgments

This study was supported in part by NIH Grants HL-113530, HL-78825, HL-55757, HL-74351, and HL-91202.

Non-standard Abbreviations and Acronyms

CPCs	cardiac progenitor cells
MI	myocardial infarction
LV	left ventricle
BrdC	5-bromo-2'-deoxycytidine
BrdU	5-bromo-2'-deoxyuridine
α-SA	α -sarcomeric Actin
FISH	fluorescent <i>in situ</i> hybridization
MACS	magnetic activated cell sorting
EF	ejection fraction
LVESV	LV end-systolic volume
LVEDV	LV end-diastolic volume
Ees	LV end-systolic elastance
PRSW	preload recruitable stroke work

REFERENCES

1. Beltrami AP, Barlucchi L, Torella D, Baker M, Limana F, Chimenti S, Kasahara H, Rota M, Musso E, Urbanek K, Leri A, Kajstura J, Nadal-Ginard B, Anversa P. Adult cardiac stem cells are multipotent and support myocardial regeneration. *Cell*. 2003; 114:763–776. [PubMed: 14505575]
2. Sanganalath SK, Bolli R. Cell therapy for heart failure: A comprehensive overview of experimental and clinical studies, current challenges, and future directions. *Circ Res*. 2013; 113:810–834. [PubMed: 23989721]

3. Keith MC, Bolli R. "String theory" of c-kit(pos) cardiac cells: A new paradigm regarding the nature of these cells that may reconcile apparently discrepant results. *Circ Res*. 2015; 116:1216–1230. [PubMed: 25814683]
4. Bearzi C, Rota M, Hosoda T, Tillmanns J, Nascimbene A, De Angelis A, Yasuzawa-Amano S, Trofimova I, Siggins RW, Lecapitaine N, Cascapera S, Beltrami AP, D'Alessandro DA, Zias E, Quaini F, Urbanek K, Michler RE, Bolli R, Kajstura J, Leri A, Anversa P. Human cardiac stem cells. *Proc Natl Acad Sci U S A*. 2007; 104:14068–14073. [PubMed: 17709737]
5. Fischer KM, Cottage CT, Wu W, Din S, Gude NA, Avitabile D, Quijada P, Collins BL, Fransioli J, Sussman MA. Enhancement of myocardial regeneration through genetic engineering of cardiac progenitor cells expressing pim-1 kinase. *Circulation*. 2009; 120:2077–2087. [PubMed: 19901187]
6. Oskouei BN, Lamirault G, Joseph C, Treuer AV, Landa S, Da Silva J, Hatzistergos K, Dauer M, Balkan W, McNiece I, Hare JM. Increased potency of cardiac stem cells compared with bone marrow mesenchymal stem cells in cardiac repair. *Stem Cells Transl Med*. 2012; 1:116–124. [PubMed: 23197758]
7. Duran JM, Makarewich CA, Sharp TE, Starosta T, Zhu F, Hoffman NE, Chiba Y, Madesh M, Berretta RM, Kubo H, Houser SR. Bone-derived stem cells repair the heart after myocardial infarction through transdifferentiation and paracrine signaling mechanisms. *Circ Res*. 2013; 113:539–552. [PubMed: 23801066]
8. Williams AR, Hatzistergos KE, Addicott B, McCall F, Carvalho D, Suncion V, Morales AR, Da Silva J, Sussman MA, Heldman AW, Hare JM. Enhanced effect of combining human cardiac stem cells and bone marrow mesenchymal stem cells to reduce infarct size and to restore cardiac function after myocardial infarction. *Circulation*. 2013; 127:213–223. [PubMed: 23224061]
9. Tang XL, Rokosh G, Sanganalmath SK, Yuan F, Sato H, Mu J, Dai S, Li C, Chen N, Peng Y, Dawn B, Hunt G, Leri A, Kajstura J, Tiwari S, Shirk G, Anversa P, Bolli R. Intracoronary administration of cardiac progenitor cells alleviates left ventricular dysfunction in rats with a 30-day-old infarction. *Circulation*. 2010; 121:293–305. [PubMed: 20048209]
10. Tang XL, Rokosh G, Sanganalmath SK, Tokita Y, Keith MC, Shirk G, Stowers H, Hunt GN, Wu W, Dawn B, Bolli R. Effects of intracoronary infusion of escalating doses of cardiac stem cells in rats with acute myocardial infarction. *Circ Heart Fail*. 2015; 8:757–765. [PubMed: 25995227]
11. Bolli R, Tang XL, Sanganalmath SK, Rimoldi O, Mosna F, Abdel-Latif A, Jneid H, Rota M, Leri A, Kajstura J. Intracoronary delivery of autologous cardiac stem cells improves cardiac function in a porcine model of chronic ischemic cardiomyopathy. *Circulation*. 2013; 128:122–131. [PubMed: 23757309]
12. Hong KU, Guo Y, Li QH, Cao P, Al-Maqtari T, Vajravelu BN, Du J, Book MJ, Zhu X, Nong Y, Bhatnagar A, Bolli R. C-kit+ cardiac stem cells alleviate post-myocardial infarction left ventricular dysfunction despite poor engraftment and negligible retention in the recipient heart. *PLoS One*. 2014; 9:e96725. [PubMed: 24806457]
13. Li Q, Guo Y, Ou Q, Chen N, Wu WJ, Yuan F, O'Brien E, Wang T, Luo L, Hunt GN, Zhu X, Bolli R. Intracoronary administration of cardiac stem cells in mice: A new, improved technique for cell therapy in murine models. *Basic Res Cardiol*. 2011; 106:849–864. [PubMed: 21516491]
14. Cai C, Guo Y, Teng L, Nong Y, Tan M, Book MJ, Zhu X, Wang XL, Du J, Wu WJ, Xie W, Hong KU, Li Q, Bolli R. Preconditioning human cardiac stem cells with an ho-1 inducer exerts beneficial effects after cell transplantation in the infarcted murine heart. *Stem Cells*. 2015
15. Leri A, Rota M, Pasqualini FS, Goichberg P, Anversa P. Origin of cardiomyocytes in the adult heart. *Circ Res*. 2015; 116:150–166. [PubMed: 25552694]
16. Hajjar RJ, Schmidt U, Matsui T, Guerrero JL, Lee KH, Gwathmey JK, Dec GW, Semigran MJ, Rosenzweig A. Modulation of ventricular function through gene transfer in vivo. *Proc Natl Acad Sci U S A*. 1998; 95:5251–5256. [PubMed: 9560262]
17. Stein AB, Tiwari S, Thomas P, Hunt G, Levent C, Stoddard MF, Tang XL, Bolli R, Dawn B. Effects of anesthesia on echocardiographic assessment of left ventricular structure and function in rats. *Basic Res Cardiol*. 2007; 102:28–41. [PubMed: 17006633]
18. Litwin SE, Katz SE, Morgan JP, Douglas PS. Serial echocardiographic assessment of left ventricular geometry and function after large myocardial infarction in the rat. *Circulation*. 1994; 89:345–354. [PubMed: 8281668]

19. Ernst C, Christie BR. Isolectin-ib 4 as a vascular stain for the study of adult neurogenesis. *J Neurosci Methods*. 2006; 150:138–142. [PubMed: 16095716]
20. Krause DS, Theise ND, Collector MI, Henegariu O, Hwang S, Gardner R, Neutzel S, Sharkis SJ. Multi-organ, multi-lineage engraftment by a single bone marrow-derived stem cell. *Cell*. 2001; 105:369–377. [PubMed: 11348593]
21. Burt RK, Chen YH, Verda L, Lucena C, Navale S, Johnson J, Han X, Lomasney J, Baker JM, Ngai KL, Kino A, Carr J, Kajstura J, Anversa P. Mitotically inactivated embryonic stem cells can be used as an in vivo feeder layer to nurse damaged myocardium after acute myocardial infarction: A preclinical study. *Circ Res*. 2012; 111:1286–1296. [PubMed: 22914647]
22. Pfeffer MA, Braunwald E. Ventricular remodeling after myocardial infarction. Experimental observations and clinical implications. *Circulation*. 1990; 81:1161–1172. [PubMed: 2138525]
23. Sutton MG, Sharpe N. Left ventricular remodeling after myocardial infarction: Pathophysiology and therapy. *Circulation*. 2000; 101:2981–2988. [PubMed: 10869273]
24. Mellough CB, Cui Q, Spalding KL, Symons NA, Pollett MA, Snyder EY, Macklis JD, Harvey AR. Fate of multipotent neural precursor cells transplanted into mouse retina selectively depleted of retinal ganglion cells. *Exp Neurol*. 2004; 186:6–19. [PubMed: 14980806]
25. Durnam DM, Anders KR, Fisher L, O'Quigley J, Bryant EM, Thomas ED. Analysis of the origin of marrow cells in bone marrow transplant recipients using a y-chromosome-specific in situ hybridization assay. *Blood*. 1989; 74:2220–2226. [PubMed: 2804360]
26. Rejman J, Colombo C, Conese M. Engraftment of bone marrow-derived stem cells to the lung in a model of acute respiratory infection by pseudomonas aeruginosa. *Mol Ther*. 2009; 17:1257–1265. [PubMed: 19417738]
27. Hong KU, Li QH, Guo Y, Patton NS, Moktar A, Bhatnagar A, Bolli R. A highly sensitive and accurate method to quantify absolute numbers of c-kit⁺ cardiac stem cells following transplantation in mice. *Basic Res Cardiol*. 2013; 108:346. [PubMed: 23549981]
28. Iso Y, Rao KS, Poole CN, Zaman AK, Curriel I, Sobel BE, Kajstura J, Anversa P, Spees JL. Priming with ligands secreted by human stromal progenitor cells promotes grafts of cardiac stem/progenitor cells after myocardial infarction. *Stem Cells*. 2014; 32:674–683. [PubMed: 24022988]
29. Anversa P, Kajstura J, Rota M, Leri A. Regenerating new heart with stem cells. *J Clin Invest*. 2013; 123:62–70. [PubMed: 23281411]
30. Leri A, Kajstura J, Anversa P. Role of cardiac stem cells in cardiac pathophysiology: A paradigm shift in human myocardial biology. *Circ Res*. 2011; 109:941–961. [PubMed: 21960726]
31. Gerbin KA, Murry CE. The winding road to regenerating the human heart. *Cardiovasc Pathol*. 2015; 24:133–140. [PubMed: 25795463]
32. Terrovitis JV, Smith RR, Marban E. Assessment and optimization of cell engraftment after transplantation into the heart. *Circ Res*. 2010; 106:479–494. [PubMed: 20167944]
33. Kemp K, Wilkins A, Scolding N. Cell fusion in the brain: Two cells forward, one cell back. *Acta Neuropathol*. 2014; 128:629–638. [PubMed: 24899142]
34. Jessberger S, Clemenson GD Jr, Gage FH. Spontaneous fusion and nonclonal growth of adult neural stem cells. *Stem Cells*. 2007; 25:871–874. [PubMed: 17185607]
35. Khan M, Nickoloff E, Abramova T, Johnson J, Verma SK, Krishnamurthy P, Mackie AR, Vaughan E, Garikipati VN, Benedict C, Ramirez V, Lambers E, Ito A, Gao E, Misener S, Luongo T, Elrod J, Qin G, Houser SR, Koch WJ, Kishore R. Embryonic stem cell-derived exosomes promote endogenous repair mechanisms and enhance cardiac function following myocardial infarction. *Circ Res*. 2015; 117:52–64. [PubMed: 25904597]

NOVELTY AND SIGNIFICANCE

What is known?

- c-kit^{POS} CPCs can be easily expanded from adult cardiac tissue.
- Short-term follow-up (< 6 weeks) studies from multiple laboratories have consistently shown that administration of CPCs promotes cardiac repair, attenuates LV dysfunction, and improves LV remodeling in various animal models of both acute and chronic post-MI heart failure.
- However, the long-term effects of CPC therapy, in terms of safety (tumor formation), fate of transplanted cells, and efficacy, are unknown.

What new information does this article contribute?

- The beneficial effects of CPCs on regional and global LV function and on LV remodeling after acute MI are sustained for at least 1 year, and thus, are likely to be permanent.
- Transplantation of CPCs is not associated with any evidence of tumor formation over the ensuing 12 months.
- Some transplanted CPCs (or their progeny) engraft and persist at 1 year after transplantation, but they fail to acquire a mature cardiomyocyte phenotype, and their number is insufficient to account for the functional and structural benefits of CPC therapy, implying that the major mode of action of CPCs is via paracrine actions.

Summary

This is the first long-term study of CPCs. Our finding that some transplanted cells persist, and continue to proliferate, at 1 year (constituting 4–8% of the nuclei) raises the possibility that their paracrine actions may be much longer-lasting than previously thought. CPC administration caused a robust and sustained (at least 12 months) proliferative response leading to formation of endogenous CPCs, endothelial cells, and small cells that express cardiac proteins (alpha-sarcomeric actin). The exact nature of these latter cells is unclear, but they do not resemble adult cardiomyocytes, even at 12 months after CPC transplantation, and thus cannot be considered cycling myocytes or myocyte precursors. This is the first evidence that transplantation of cells (of any type) in the heart induces a sustained proliferative response that lasts at least 12 months. While the mechanism for this phenomenon remains to be elucidated, its occurrence offers a plausible explanation for the seemingly paradoxical observation that the salutary effects of cell therapy persist even after the transplanted cells have disappeared. The data are consistent with a paradigm in which exogenous CPCs activate endogenous CPCs and other cells, which proliferate and promote cardiac repair. The long-term safety and efficacy of CPCs observed in this study provide a strong rationale for clinical translation.

Experimental Protocol

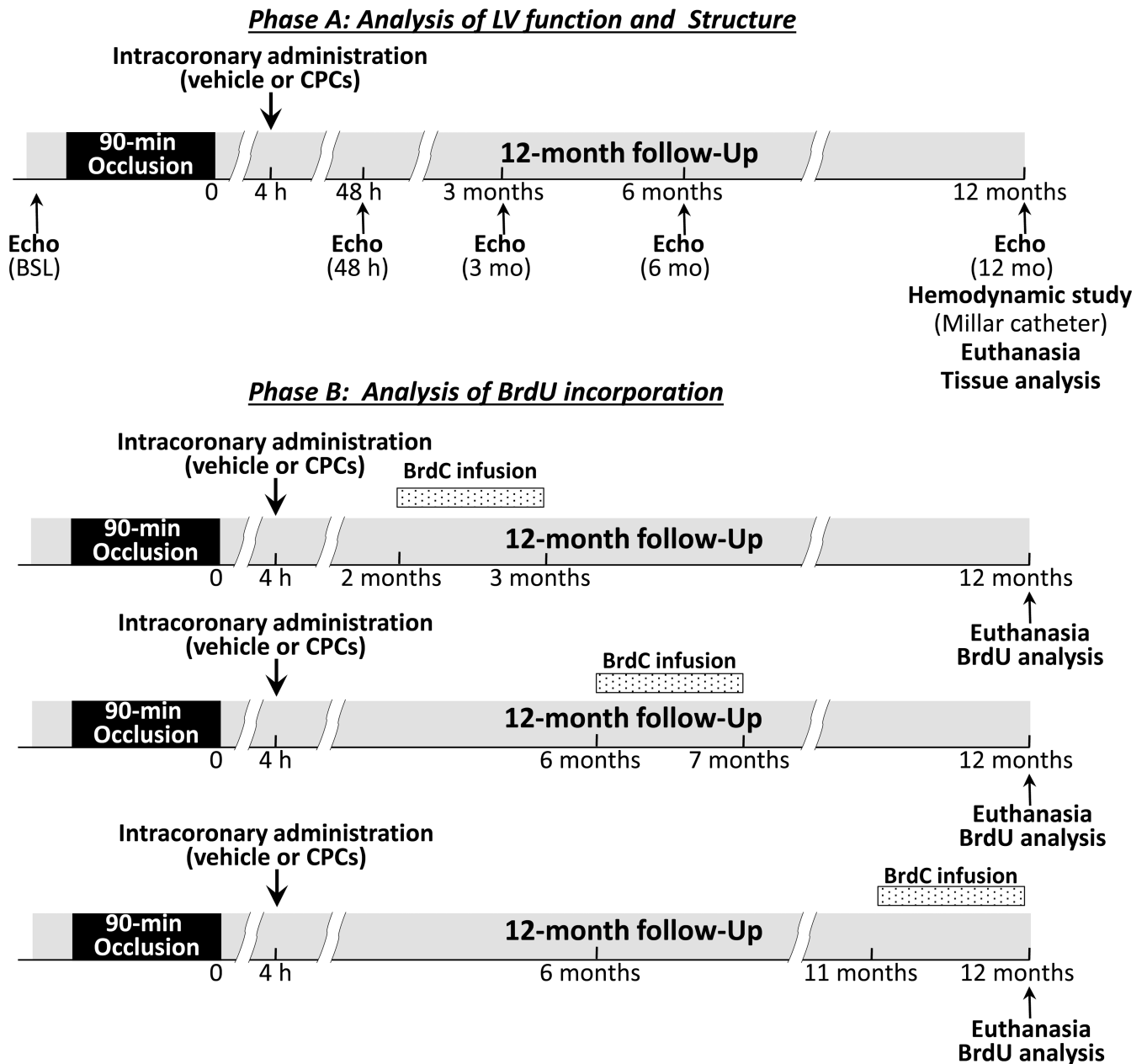


Figure 1. Experimental protocol

Rats were subjected to a 90-min coronary occlusion followed by reperfusion; four hours after reperfusion, they received intracoronary infusion of either vehicle or CPCs. Rats were followed up for 12 months. **Phase A:** *Analysis of LV function and structure.* Echocardiographic studies were performed at baseline (BSL), 48 h, and 3, 6, and 12 months after MI. Hemodynamic studies were performed immediately before euthanasia at the 12-month follow-up. Hearts were perfused and fixed with formalin for histology and Y-chromosome analysis. **B.** *Analysis of BrdU incorporation.* Rats received a 1-month BrdC

infusion via an osmotic pump starting at 2, 6, or 11 months after intracoronary CPC administration; animals were euthanized for assay of BrdU incorporation at 12 months after CPC administration.

Author Manuscript

Author Manuscript

Author Manuscript

Author Manuscript

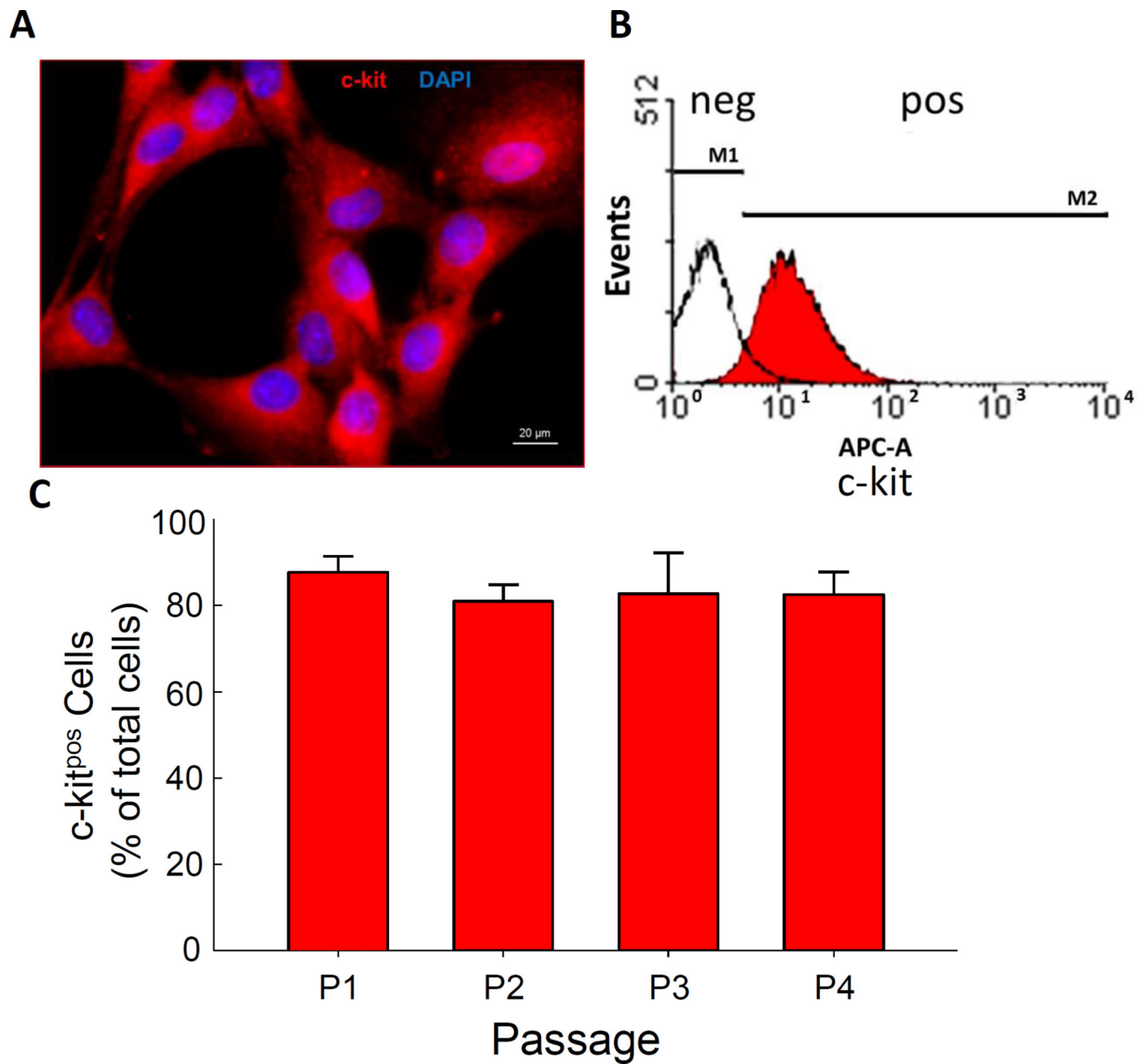


Figure 2. Rat c-kit^{pos} CPCs

A. CPCs were stained for c-kit and visualized by confocal microscopy; **B.** c-kit^{pos} CPCs were stained for c-kit and the c-kit^{pos} population identified by flow cytometry; **C.** Quantitation of c-kit^{pos} CPCs in passages 1 to 4 in culture after magnetic sorting. Data are means \pm SEM.

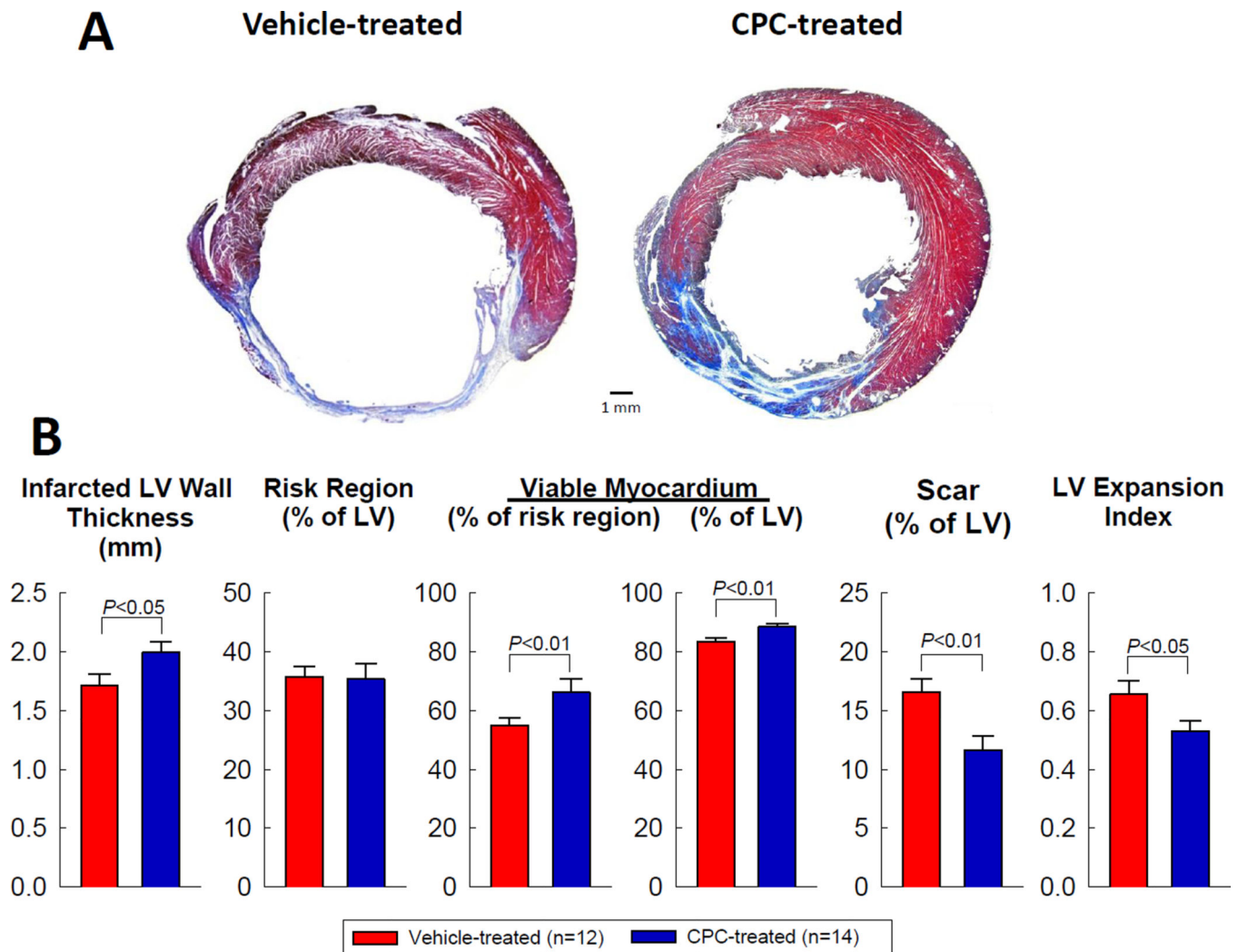


Figure 3. Morphometric assessment of LV remodeling

A. Representative Masson's trichrome-stained myocardial sections from a vehicle-treated and a CPC-treated heart. Scar tissue and viable myocardium are identified in blue and red, respectively. Note that the LV cavity is smaller and the infarcted wall thicker in the CPC-treated heart. **B.** Quantitative analysis of LV morphometric parameters, including infarcted LV wall thickness, weight of risk region (as % of the total LV weight), weight of viable myocardium (both as % of risk region weight and total LV weight), weight of scar tissue (as % of the total LV weight), and LV expansion index. Data are means \pm SEM.

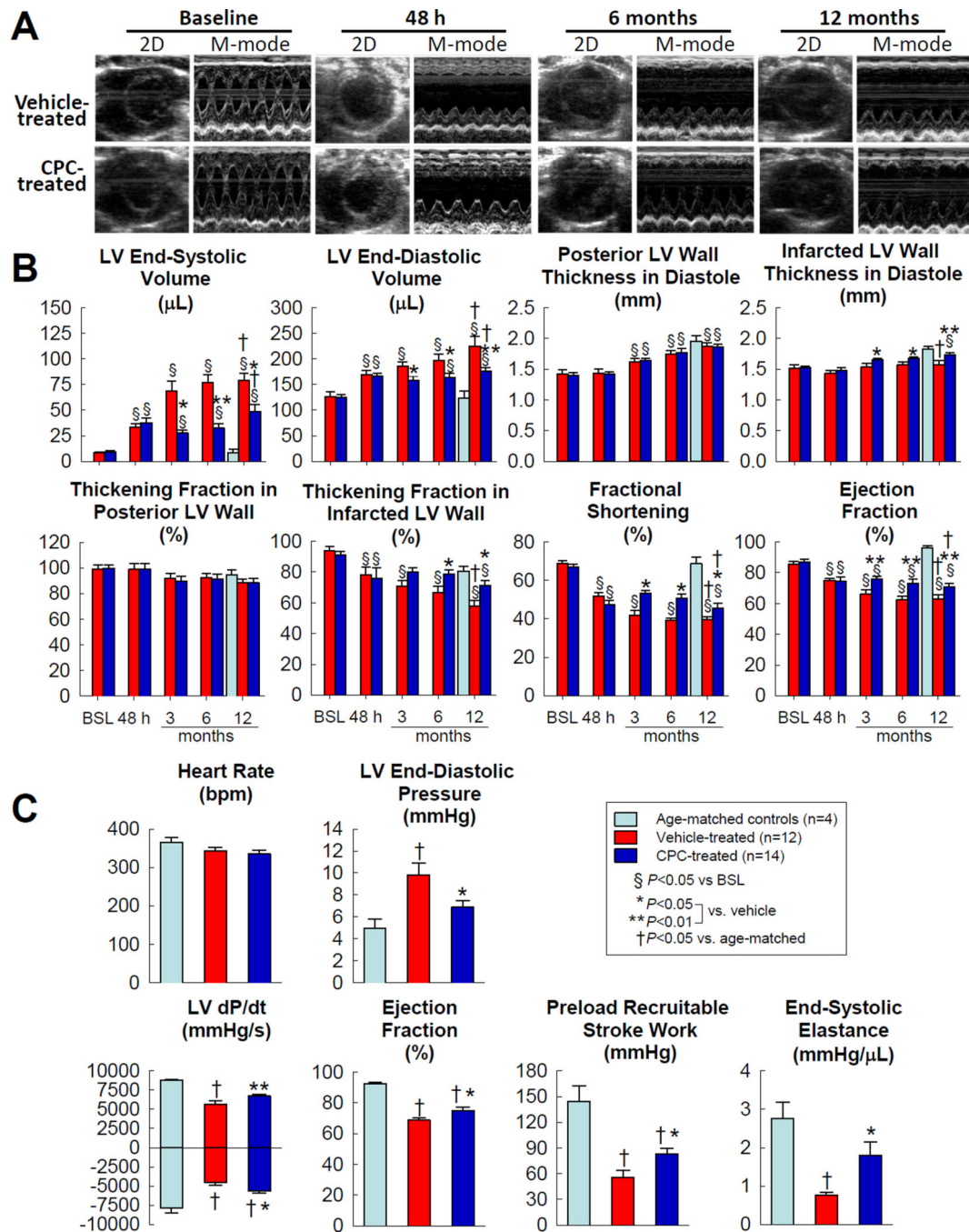


Figure 4. Echocardiographic and hemodynamic assessment of LV dimensions and function

A. Representative 2D and M-mode echocardiographic images from a vehicle and a CPC-treated rat recorded at baseline (BSL) and at 48 h, 6 months (6-mo), and 12 months (12-mo) after MI. **B.** Quantitative analysis of echocardiographic parameters. **C.** Hemodynamic assessment of LV function at 1 year follow-up. To facilitate comparisons, four normal (noninfarcted) age-matched rats were studied at the 12-month follow-up time point. Data are means \pm SEM.

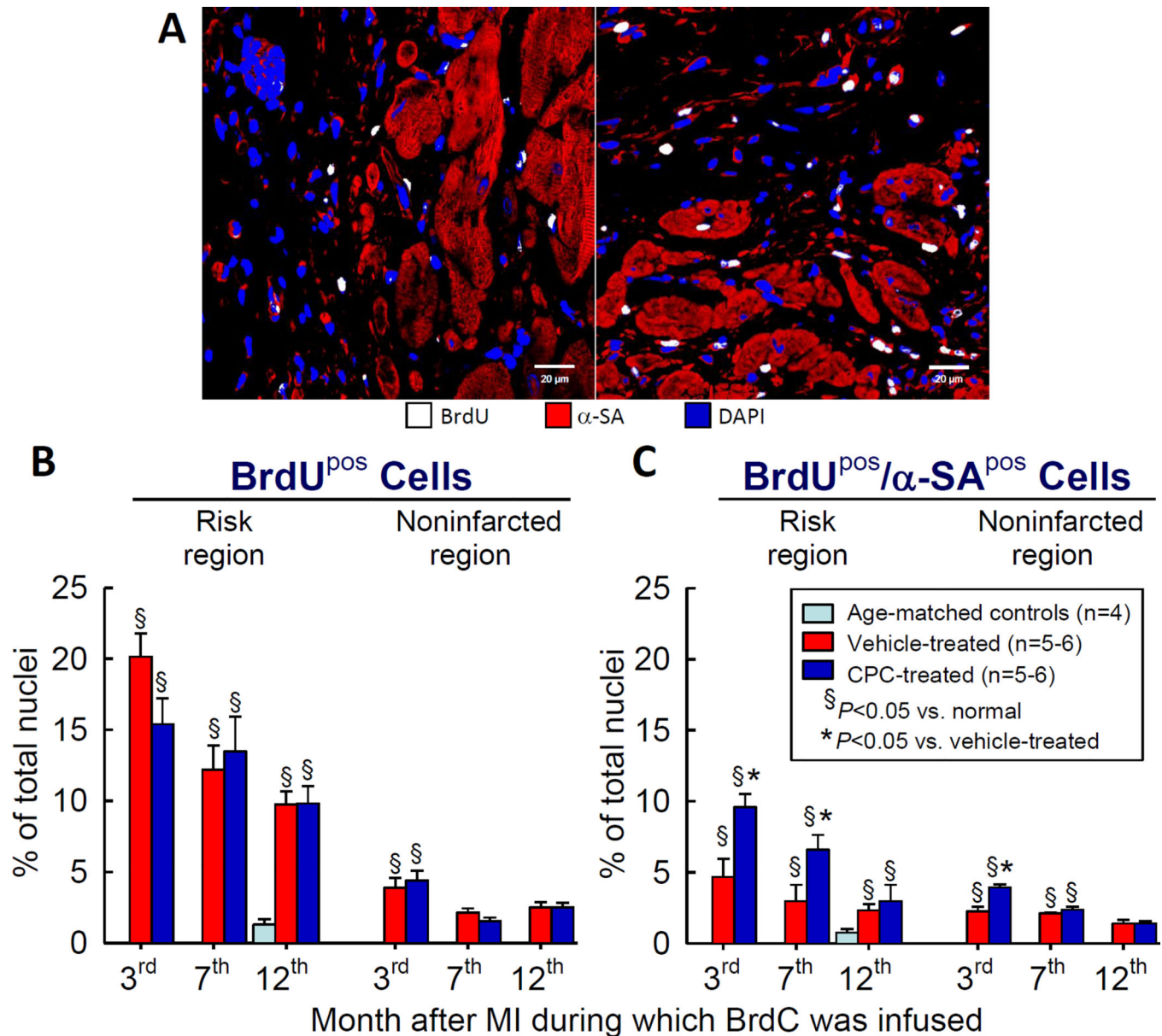


Figure 5. Analysis of BrdU incorporation

A. Representative confocal microscopic images of LV sections from a vehicle and a CPC-treated rat that received BrdC infusion in the 3rd month after MI. **B.** Quantitative analysis of total BrdU^{pos} cells and BrdU^{pos}/α-SA^{pos} cells in the risk region and noninfarcted region (posterior wall) of rats that received BrdC infusion in the 3rd, 7th, or 12th month after MI. To facilitate comparison, four normal (noninfarcted) age-matched rats received BrdC infusion for 1 month at a time equivalent to the 12th month after MI. Data are means ± SEM. The region at risk comprises both the border zones and the scarred region.

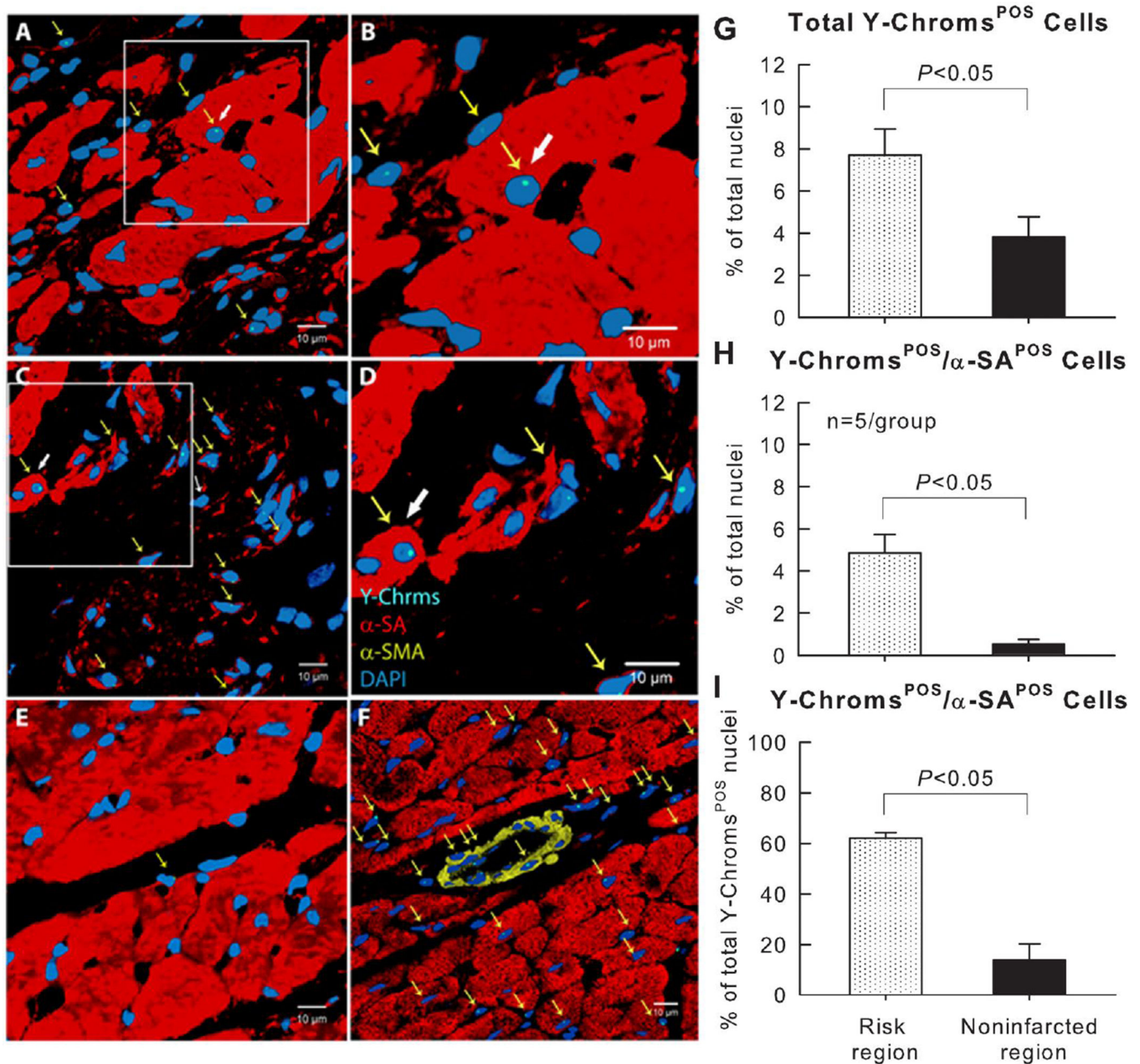


Figure 6. Fluorescence *in situ* hybridization (FISH) for detection of Y-chromosome 1 year after cell transplantation

A–E. Positivity for Y-chromosome in representative confocal microscopic images obtained from the border zone (**A, B**), scarred region (**C, D**), and noninfarcted region (**E**) identifies exogenous CPCs. Yellow arrows indicate all Y-chromosome positive cells, whereas white arrows indicate Y-chromosome cells with a myocyte-like appearance. **B** and **D** are higher magnification images of the boxes in **A** and **C**, respectively. **F.** Male heart tissue (positive control); Y-chromosome fluorescent signals are not present in all nuclei because some signals are out of the plane of focus used for the image. Y-chromosome (Y-Chrms) is shown in cyanine blue, α-sarcomeric actin (α-SA) in red, α-smooth muscle actin (α-SMC) in

yellow, and nuclei are stained with DAPI (blue). **G–I.** Quantitative analysis of the number of Y-chromosome/ α -SA double positive cells at 1 year after CPC transplantation. Data are means \pm SEM. The region at risk comprises both the border zones and the scarred region. Bars are 10 μ m.

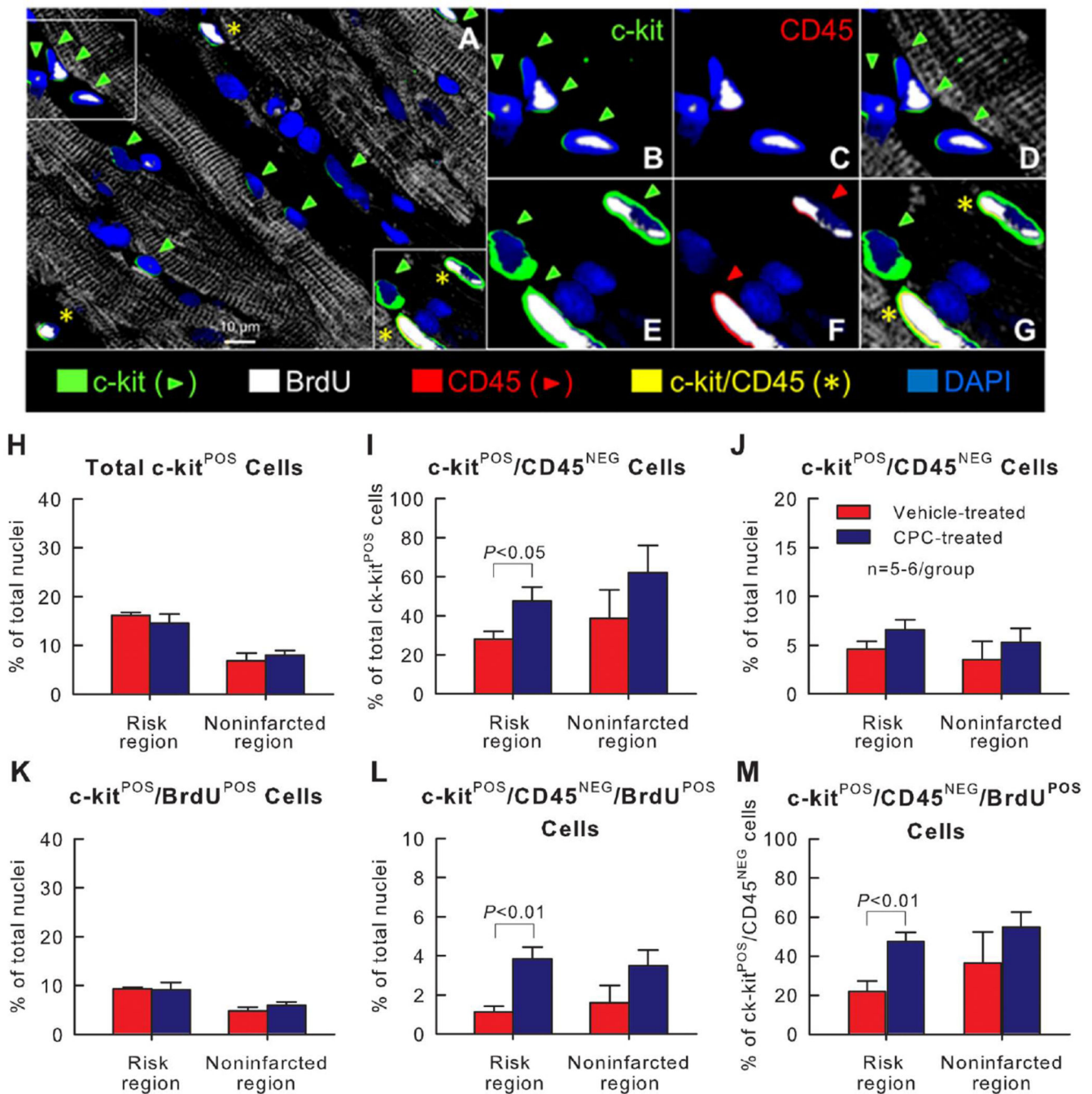


Figure 7. Analysis of CPCs (c-kit^{POS}/CD45^{POS} cells) 1 year after cell transplantation

A. Representative confocal microscopic image obtained from the border zone (a larger version of this figure is presented in Supplementary Fig. 6). **B, C, and D** are higher magnification images of the upper-left box in **A**; **E, F, and G** are higher magnification images of the lower-right box in **A**. Green arrowheads indicate c-kit^{POS}/CD45^{NEG} cells (i.e., CPCs), whereas yellow asterisks indicate c-kit^{POS}/CD45^{POS} cells (i.e., hematopoietic stem cells). C-kit expression is shown in green, BrdU in white, and CD45 in red; c-kit/CD45 double positive cells are yellow, myocyte morphology is shown in gray/white, and nuclei are

blue (DAPI). Myocardial morphology was examined with the confocal ChD detector under transmitted light, in which the pseudocolor selected for the ChD channel was gray white. **H–M.** Quantitative analysis of the number of c-kit^{POS}/BrdU^{POS} cells (new c-kit^{POS} cells formed during the 12th month after MI) and c-kit^{POS}/CD45^{NEG}/BrdU^{POS} cells (new CPCs formed during the 12th month after MI) at 1 year after CPC transplantation. Data are means \pm SEM. RR, risk region; NR, noninfarcted region. The region at risk comprises both the border zones and the scarred region. Bar is 10 μ m.

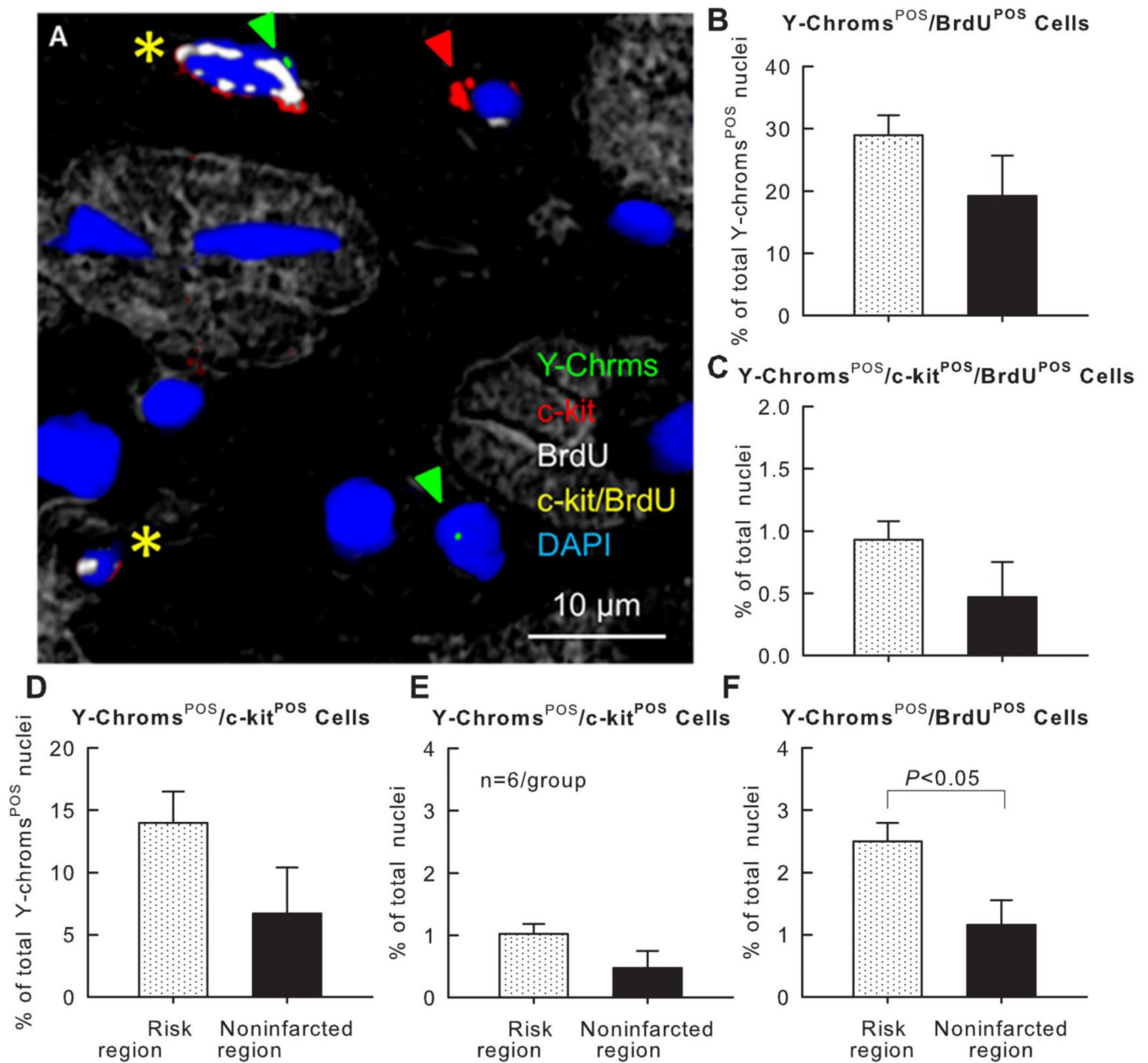


Figure 8. Analysis of Y-chromosome^{POS}, c-kit^{POS}, and BrdU^{POS} cells 1 year after cell transplantation

A. Representative confocal microscopic image obtained from the scarred region (a larger version of this figure is presented in Supplementary Fig. 7). Green arrowheads indicate Y-chromosome fluorescent signals (green/cyan) in nuclei. Positivity for c-kit is shown in red and for BrdU in white. Nuclei are stained with DAPI (blue). Yellow asterisks indicate c-kit and BrdU double positive cells. The red arrowhead indicates a c-kit positive, BrdU negative, and Y-chromosome negative cell. **B – F.** Quantitative analysis of the number of Y-chromosome^{POS}, c-kit^{POS}, and BrdU^{POS} cells 1 year after CPC transplantation. Data are

means \pm SEM. RR, risk region; NR, noninfarcted region. The region at risk comprises both the border zones and the scarred region. Bar is 10 μ m.

Author Manuscript

Author Manuscript

Author Manuscript

Author Manuscript

Table 1

Body weight and postmortem measurements of LV weight and LV length

	Age-matched normal controls (n=4)	Vehicle-treated (n=12)	CPC-treated (n=14)
Body weight (g) at baseline	171.5±3.8	196.3±4.1^a	188.2±3.4^a
% gain from baseline at 3-month follow-up	--	7.9±2.3	18.7±1.5 ^{**}
% gain from baseline at 6-month follow-up	--	20.0±3.2	27.1±1.7 [*]
% gain from baseline at 12-month follow-up	--	37.7±3.1	47.6±2.8 [*]
LV weight (g) at the end of the 12-month follow-up	0.72±0.02	1.00±0.03^a	0.91±0.03^{*a}
LV length (mm) at the end of the 12-month follow-up	10.5±0.6	15.1±0.4^a	13.0±0.5^{**a}
LV weight/body weight ratio	0.27±0.01	0.37±0.01^a	0.33±0.01^{*a}

Data are means ± SEM.

^{*}
P<0.05,^{**}
P<0.01 vs. vehicle;^a
P<0.05 vs. age-matched normal controls

Table 2

Morphometric analysis

	Vehicle-treated (n=12)	CPC-treated (n=14)
LV weight at postmortem measurement (mg)	995.8 ±30.3	914.3±29.8
Area measured by trichrome image analysis		
LV area (mm ²)	48.2±3.1	47. 6±2.4
Risk area (mm ²)	17.3±1.6	17.0±1.7
Scar area (mm ²)	8.0±0.8	5.4±0.6 *
Non-risk area (mm ²)	30.8±1.9	30.6±1.7
Weight calculated from area measured by trichrome analysis		
Risk region weight (mg)	352.8±16.1	322.4±27.0
Scar tissue weight (mg)	162.5±9.3	103.3±9.4 **
Non-risk region weight (mg)	643.0±31.8	591.9±31.6
Viable tissue weight within risk region (mg)	190.3±14.3	219.1±26.5
Total viable tissue in LV (mg)	833.3±33.2	811.0±33.6
Percentages calculated from weight		
Risk region weight (% of LV weight)	35.7±1.8	35.3±2.6
Scar tissue weight (% risk region weight)	46.4±2.4	34.2±3.0 **
Scar tissue weight (% of LV weight)	16.6±1.1	11.6±1.2**
Viable tissue weight (% risk region weight)	53.6±2.4	65.8±3.0**
Viable tissue weight (% of LV weight)	83.4±1.1	88.4±1.2 **

Data are means ± SEM.

* $P<0.05$,

** $P<0.01$ vs. vehicle-treated